Original Article
A novel tetrapeptide for chelator-free radiolabeling in optimized preparation of 99mTc-radiolabeled oligonucleotides

Zhao Chen[1*], Qi Yang[1*], Lele Song[1], Yongkang Qiu[1], Sitong Wu[2], Wenpeng Huang[1], Qiao Jiang[1], Shengnan Wu[1], Lei Kang[1]

Departments of [1]Nuclear Medicine, [2]Interventional Radiology and Vascular Surgery, Peking University First Hospital, Beijing 100034, China. *Equal contributors.

Abstract: Antisense imaging uses radionuclide labeled antisense oligonucleotides to hybridize with nucleic acids in vivo, display the expression of target genes, and directly quantify biological processes at the cellular and subcellular levels. The anti-miRNA oligonucleotides (AMOs) are a series of single-stranded DNA oligonucleotides that are widely used in gene imaging and gene therapy. However, due to the negative charge and high molecular weight, the permeability through the membrane of AMOs is generally low so that most AMOs cannot enter the cells. Based on the 99mTc-labeled AMOs imaging in previous studies, this study developed a novel tetrapeptide Glycine-Alanine-Glycine-Lysine (Gly-Ala-Gly-Lys, GAGK) for one-step labeling AMO with 99mTc. The labeling conditions were optimized by changing the number of stannous ions, the reaction time, and the temperature, respectively. The labeled products were identified by gel electrophoresis and their serum stability was evaluated. The optimal labeling condition in this study was using 1 mg/mL $SnCl_2 \cdot 2H_2O$ and heating for 30 min at 100°C. Gel electrophoresis confirmed the verification of successful labeling of 99mTc-GAGK-AMO. After being incubated with human fresh serum for 12 h, 99mTc-GAGK-AMO showed good stability and no obvious degradation. Therefore, this labeling method has high labeling efficiency and stable labeling, which provides an effective method for the application of miRNA-targeted imaging.

Keywords: Peptide, glycine-alanine-glycine-lysine (Gly-Ala-Gly-Lys, GAGK), 99mTc, radiolabel, anti-miRNA oligonucleotides (AMOs)

Introduction

Cancers are malignant diseases, which seriously endanger human health and quality of life. Nuclear medicine uses radionuclide tracer technology for molecular imaging, which has advantages in tumor imaging because of its high sensitivity, specificity, and non-invasive characteristics. In recent years, there have been many studies on radionuclide-labeled imaging for different targeted biomolecules [1, 2]. Radionuclides used for labeling need to be selected according to the energy released during the decay process, half-life, and chemical form. Among these radionuclides, technetium-99m (99mTc) has been commonly used in the clinic because of its wide availability and favorable physical features.

Antisense imaging is the application of radioactive labeling technology to antisense theory. It uses radionuclide labeled antisense oligonucleotides to hybridize with nucleic acids in vivo, display the expression of target genes, and directly express and quantify biological processes at the cellular or subcellular level [3-5]. MicroRNA (miRNA) is a kind of endogenous non-coding single-stranded RNA with a low molecular weight, which generally has 20 to 24 nucleotides. They can target specific messenger RNA (mRNA) to inhibit translation or to regulate at the post-transcriptional level and cause specific degradation [6]. Direct imaging of overexpressed mRNA can provide information on gene expression patterns at the cell level, and reveal molecular changes in the relatively early stage of the disease [7]. When the expression of some miRNAs is abnormal due to gene deletion, amplification, variation, and other reasons, it may lead to malignant tumors. However, the most commonly used detection method for

miRNA is the pathological examination, which is invasive and may appear false negative. Therefore, to detect miRNA noninvasively and achieve early diagnosis of tumors, it is necessary to develop a method that can detect miRNA expression in vivo. Previous studies have shown that one of the necessary methods to detect miRNA is to use antisense nucleic acids, which are based on base pairing interactions [8]. To study the application of miRNAs, synthetic anti-miRNA oligonucleotides (AMOs) have complementary sequences with mature miRNAs. AMO can specifically bind to their targeted miRNA and cause gene expression to be suppressed [9]. MiRNA-21 has been considered one of the most important miRNAs and is overexpressed in many tumors [10]. AMO-21 can be regarded as a potential probe for targeting miRNA-21 in vitro and in vivo.

Oligopeptides have the advantages of low molecular weight and low toxicity. It has been widely used and studied in materials science, molecular imaging, and carrier studies for disease diagnosis and treatment [11]. Some studies reported that using the oligopeptide of four amino acids Glycine(D)-Alanine-Glycine-Glycine (Gly(D)-Ala-Gly-Gly, GAGG), a strong chelating residues structure similar to the N4 structure which could be used for labeling ^{99m}Tc [4, 12]. To eliminate space hindrance, γ-Aminobutyric acid (Aba) is used as a spacer to chelate ^{99m}Tc. However, its labeling stability is not satisfactory [12]. In this study, we designed a novel tetrapeptide sequence of Glycine-Alanine-Glycine-Lysine (Gly-Ala-Gly-Lys, GAGK) which was used to label AMO-21 with ^{99m}Tc and optimized the labeling conditions and serum stability.

Materials and methods

Oligonucleotides

AMO-21 is a single-stranded DNA oligonucleotide that can bind with mature miRNA-21 [13]. To improve binding stability and affinity, we modified 2'-O-methyl (2'-OMe) bases and phosphorothioate linkage bases at each end of AMO [14]. AMO-21 (5'-TCAACATCAGTCTGTGTGATAA-GCTA-3') were synthesized by Shanghai Science Peptide Biological Technology Co. Then the products were purified by reversed-phase high-performance liquid chromatography (HPLC) with a C18 column (Waters, SunFire 100 A, 5 μm, 4.6 × 250 mm). The elution gradient was

from 20% to 40%, with acetonitrile and 0.1 M tetraethylammonium bromide in water as the gradient at the 1.5 mL/min elution flow rate. A mass spectrometer (Shimadzu-Kratos AXIMA-CFR PLUS TOF) was used to analyze the product mass spectra of Matrix-assisted laser desorption/ionization time-of-flight (MALDI-TOF). All oligonucleotides with modification were stored at -80°C after the purification and verification.

Design and synthesis of GAGK

This study designed a novel peptide sequence of Gly-Ala-Gly-Lys (GAGK) for radiolabeling with ^{99m}Tc. Tetrapeptide of GAGK was linked to the 3' end of AMO-21 with the sequence of 3'-GAGK-ATCGAATAGTCTGACTACAACT-5'. 3'-end was chosen as the linked site by avoiding affecting the activity of the nucleic acid probe. The N4-like structure formed by four amino acids provides 4-5 coordination electrons to form strong chelating residues to chelate ^{99m}Tc. All GAGK peptides were synthesized by Shanghai Sangon Biological Engineering (China), then purified and modified as before.

Radiolabeling

^{99m}Tc radiolabeling was performed according to the previous study [15]. In brief, fresh SnCl$_2$·2H$_2$O were dissolved in ascorbic HCl (10 mM). 0.5 M sodium bicarbonate, 0.25 M ammonium acetate, and 0.175 M ammonium hydroxide were used to prepare sodium tartrate buffer (50 mg/mL, pH 9.2). Lyophilized GAGK peptide conjugated product (4 nmol) was dissolved in this buffer (15 μL) with ammonium acetate solution (40 μL 0.25 M) to a final pH of 8.0-8.5. Different concentrations of fresh SnCl$_2$·2H$_2$O (5 μL) were added following the addition of fresh ^{99m}Tc-pertechnetate solution (15 μL), which was produced by the China Institute of Atomic Energy. The amount of sodium pertechnetate required for labeling typically depended on the purpose of the labeling.

Labeling optimization

Labeling conditions were optimized by adjusting concentrations of SnCl$_2$·2H$_2$O, reaction temperature, and reaction time. For different concentrations of fresh SnCl$_2$·2H$_2$O (1, 2, 4, 8 mg/mL), different temperatures (100°C and room temperature), and different heating duration (0, 5, 15, 30, 45, 60 min), ^{99m}Tc-radiolabeled
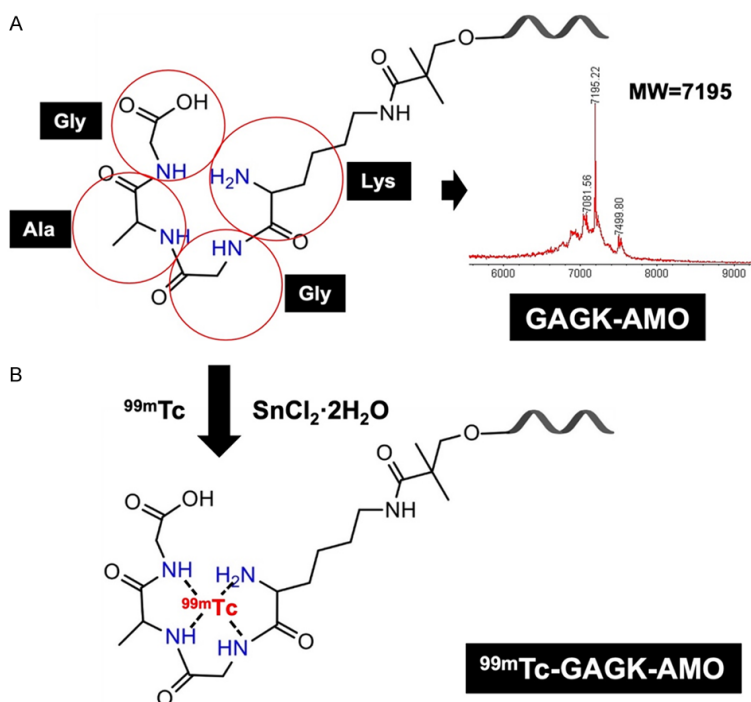
Figure 1. Scheme of ^{99m}Tc-GAGK-AMO. A. The molecule weight of GAGK-AMO was 7195.22 which was measured by mass spectroscopy. B. The tetrapeptide sequence of GAGK provides the Coordination bonds for ^{99m}Tc radiolabeling.
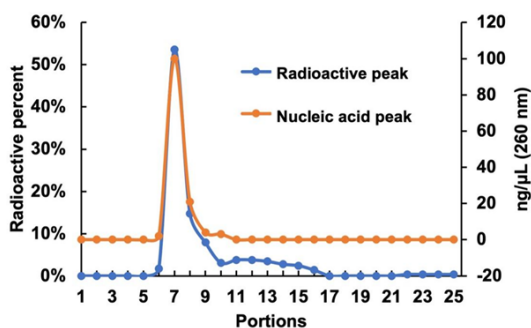
Figure 2. Radioactive distribution and 260 nm absorbance results of different portions after purification with a Sephadex G25 column. The radioactivity and 260 nm absorbance peak tubes are located in the same portions.

GAGK-AMO were measured by radio-TLC and purified using Sephadex G25 column. TLC was performed using silica gel GF-254 coated on glass plates (Analtech Inc.). Finally, the absorbance value and radioactivity at 260 nm were measured.

Agarose gel electrophoresis

The function of agarose gel electrophoresis was to identify the accuracy and integrity of the radiolabeled product. Unlabeled GAGK-AMO, ^{99m}Tc-GAGK-AMO, ^{99m}Tc-pertechnetate were loaded on agarose gel (2%) respectively and then analyzed after running 20 min at 200 V. The agarose gel was stained by GV-2 staining reagents (Beijing SBS Genetech). Oligonucleotide bands were visualized under ultraviolet light at 300 nm using a gel imaging analyzer. Then the gel was divided into equal portions and a NaI scintillation detector (Perkin-Elmer) was used to measure their corresponding radioactive counts. A SPECT (Discovery NM/CT 670, GE Healthcare) was used to scan the radiograph.

Serum stability

^{99m}Tc-GAGK-AMO was incubated in fresh human serum (0.01 mg/mL) for 12 h at room temperature to evaluate the in vitro labeling stability. At 0, 1, 2, 4, 6, 8, 10, and 12 h, ^{99m}Tc-GAGK-AMO was tested respectively by agarose gel electrophoresis to measure its ability against degradation in human serum. The gels were also evaluated by gel imaging and radioactive counts in different portions as described above.

Results

Radiolabeling of AMO

After the tetrapeptide GAGK was linked at 3' end of AMO-21, mass spectroscopy was used to test the molecule weight of the GAGK-AMO products. The measured molecular weight was 7195.22, which was consistent with the expected one (**Figure 1A**). GAGK-AMO was then radiolabeled by ^{99m}Tc successfully via the tetrapeptides sequence providing 4-5 coordination electrons to form strong chelating residues (**Figure 1B**). The radioactivity of radiolabeled products was measured after purification. The radioactivity peak of radiolabeled products was correlated with the nucleic acid peak at 260 nm, suggesting the successful labeling (**Figure 2**). The radioactivity peak was solely displayed with the labeling rate at about 90.03%±4.16%
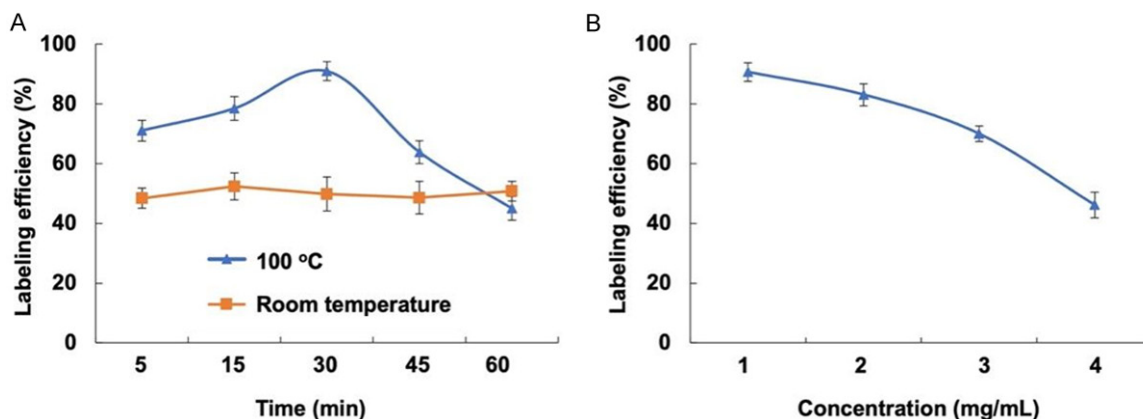
Figure 3. Optimization of radiolabeling condition. (A) Reaction time with/without heating and (B) concentration of SnCl$_2$·2H$_2$O were optimized and showed the radioactivity efficiency reached 90.03%±4.16% under the optimal reaction conditions with 1 mg/mL concentration of SnCl$_2$·2H$_2$O and heating for 30 min.

and the specific activity at 32.25±7.6 μmCi/ μmol (n=5). After purifying with Sephadex G25, ^{99m}Tc-labeled oligonucleotides were tested for their radioactivity and absorbance at 260 nm. The recovery rate of oligo after each labeling reaction was more than 90% with the average concentration at 42.8±6.8 ng/μL.

Radiolabeling efficiency using different reaction time

Different reaction times (5, 15, 30, 45, and 60 min) at 100°C or room temperature affected the labeling efficiency. For the optimization of the labeling in this study, we used 200-300 μCi fresh sodium pertechnetate in 15 μL, whereas we will add more sodium pertechnetate with a higher concentration for the labeling for animal studies. The specific activity should be more than 32.3 μCi/nmol. Different labeling efficiency of labeled products was obtained under different heating conditions. After heating for 15 min, the labeling efficiency was higher than 78.46%±4.00%, and heating for 30 min got the highest labeling efficiency (90.03%±4.16%). But, prolonging reaction time by more than 30 min decreased rather than improve the radiolabeling efficiency, suggesting that heating for 30 min can be used to shorten the radiolabeling time. The radiolabeled efficiency dropped to 45.00%±3.97% at 60 min. Without heating, no more labeled products can be obtained by prolonging the reaction time (**Figure 3A**).

Radiolabeling efficiency under different temperature

Different temperatures (100°C and room temperature) also affected the labeling efficiency.

The radiolabeling efficiency after heating is higher than that at room temperature whereas the highest labeling rate at room temperature was about only 52.40%±4.55% (**Figure 3A**). Therefore, 30 min and 100°C were chosen as the optimized heating condition because of the high labeling efficiency.

Radiolabeling efficiency using different concentrations of SnCl$_2$·2H$_2$O

The concentration of SnCl$_2$·2H$_2$O is also an important factor in ^{99m}Tc-radiolabeled reaction. The labeling rate of SnCl$_2$·2H$_2$O at the concentration of 1 mg/mL is about 90.67%±3.13% reaching the highest labeling efficiency. In the comparison, high concentrations of stannous lead to decreased labeling efficiency, from 83.10%±3.72% to 46.17%±4.30%. As the concentration of SnCl$_2$·2H$_2$O Increased, the labeling efficiency was reduced (**Figure 3B**). Excessive stannous may lead to unnecessary technetium colloid, thus reducing the labeling efficiency. Therefore, using SnCl$_2$·2H$_2$O of 1 mg/mL concentration and heating for 30 min was chosen for the optimized labeling condition in this study.

Verification of radiolabeling

Gel electrophoresis was to show the position and situation of GAGK-AMO before and after labeling with ^{99m}Tc. The results of gel imaging showed that GAGK-AMO bands were clear and were located at the same position before and after ^{99m}Tc labeling, suggesting there is no effect in the labeling process (**Figure 4A**, left panel). After being imaged by SPECT, the GAGK-AMO band showed obvious radioactive distribu-
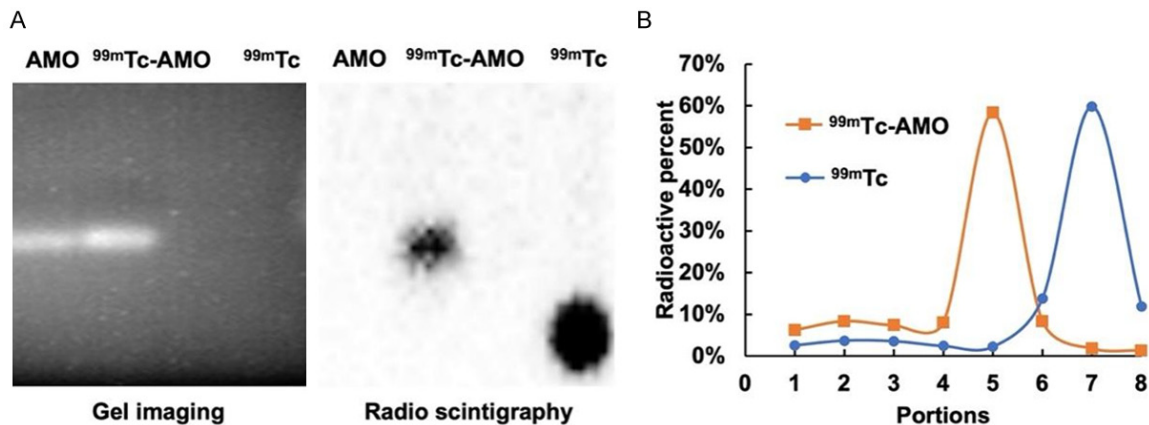
Figure 4. Verification of ^{99m}Tc-GAGK-AMO. A. The results of gel imaging and radio scintigraphy after gel electrophoresis showed radioactive distribution was consistent with the location of ^{99m}Tc-GAGK-AMO. B. Radioactive counts were measured after dividing the gel into equal portions and confirmed the successful AMO labeling.
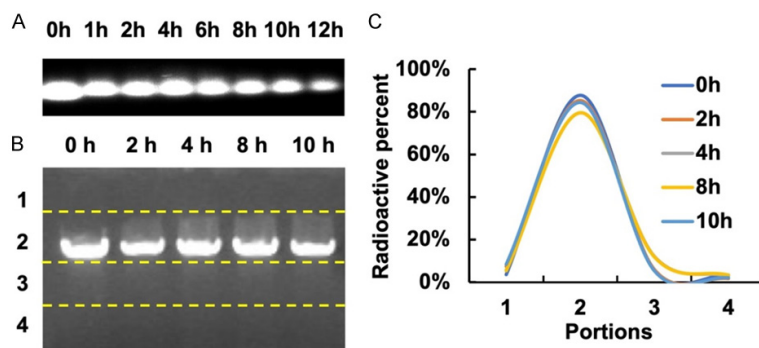
Figure 5. Serum stability of ^{99m}Tc-GAGK-AMO. (A) Gel electrophoresis showed clear bands within 12 h. Radiolabeling stability was shown by (B) gel electrophoresis and (C) radioactive percent measurement. The radioactive peak was consistent with the position of AMO bands in the gel, confirming good stability of ^{99m}Tc-GAGK-AMO within 10 h.

tion in the same position as the band in the gel. ^{99m}Tc-pertechnetate showed radioactive distribution ahead of the position of AMO due to the small molecular weight (**Figure 4A**, right panel). After dividing the gel into equal portions, an obvious radioactivity peak was found at the 5th portion which was corresponding to the nucleic acid band whereas the ^{99m}Tc-pertechnetate radioactive peak was located at the 7th portion (**Figure 4B**). The above results confirmed that ^{99m}Tc-GAGK-AMO labeling was successful.

Stability in serum

The probe was incubated in fresh human serum for 0, 1, 2, 4, 6, 8, 10, and 12 h respectively to observe the serum stability. Observed by gel electrophoresis, the radiolabeled AMO presented a single and clear band in the gel within 12 hours, suggesting the relative stability of AMO in serum. Although the band brightness decreased slightly over time relating to the possible degradation in serum, considering that it was pure serum and the probe has not been modified to improve its stability, the serum stability of the probe was acceptable (**Figure 5A**). Furthermore, we tried diluted serum as the incubated medium (10% human fresh serum). The results of labeling stability measurement showed that the labeled products had no obvious degradation within 10 h in diluted serum, the band brightness was uniform, and the radioactivity at the band was at the peak of gel. There was no radioactivity peak at other positions (**Figure 5B**). The above results showed that the labeled probe has good labeling stability and serum stability, and there is no obvious off-labeling phenomenon.

Discussion

With the successful application of antisense imaging and radionuclide tracer technology, molecular-level accurate tracer technology is gradually used in tumor localization and treatment. ^{99m}Tc is the most commonly used radionuclide in clinic nuclear medicine so far, which

has the advantages of a pure γ ray emitter, with appropriate half-life and ray energy, simple acquisition, and low cost. It has been widely used in the clinic, and it is also an ideal radionuclide for labeling drugs. The methods of ^{99m}Tc labeling AMOs include direct labeling and indirect labeling. At present, the commonly used method is the indirect labeling method using a bifunctional chelator (BFCA). The earliest BFCA used in antisense imaging is diethylene triamine pentaacetate acid (DTPA) [16], but its labeling rate and specific activity are low, and the product is unstable [17], which is gradually replaced by other BFCAs. At present, commonly used BFCAs include hydrazinonictinamide (HYNIC), N-hydroxysuccinimide derivative of S-acetylmercaptoacetyltriglycine (NHS-MAG3), etc. However, the labeling rate using chelating agents is affected by the coupling results. To solve this problem, this study tries to develop a direct labeling method by using a tetrapeptide sequence GAGK to achieve miRNA radiolabeling of ^{99m}Tc. We obtained a high labeling rate by different reaction conditions optimization, and confirmed the reliability and stability of labeling in vitro, providing a new idea for ^{99m}Tc radiolabeling AMOs.

Tetrapeptide can be regarded as a derivative of MAG_3, in which amino acid residues replace mercaptoacetyl residues. Previous animal experiments have proved that ^{99m}Tc-GAGG has a renal excretion rate similar to ^{99m}Tc-MAG3, which can be excreted quickly through urine and is rarely absorbed in the liver and other organs [18]. These results showed that the ^{99m}Tc-peptide-AMOs probe can be used for tumor gene expression imaging if tumor uptake can be enhanced. At present, the commonly used method is the indirect labeling method using BFCA, therefore, for labeling, two steps should be needed. The efficiency of conjugation between chelators and probes can affect the labeling efficiency to a large extent. One-step labeling method using peptide coupling could overcome this shortage and provide some other advantages, including ready-to-label preparation, less operation, long-term storage, and easier use for kits [19]. Therefore, based on the structural advantages, using a short peptide structure to mediate ^{99m}Tc labeling is now a research hotspot, but there is no study on ^{99m}Tc labeling AMO-21 with peptide sequence.

Due to the low molecular weight of miRNA, antisense oligonucleotides are considered to be the best measurement tool for targeting miRNA [20]. Therefore, radiolabeled probes based on AMOs are widely used in gene imaging and gene therapy [21]. AMOs have 15 to 25 nucleotide complementary single chains which can bind to the target gene. Studies have shown that after chemical synthesis and modification of AMOs, the plasma binding protein affinity of AMOs increases, and the nuclease degradation rate of AMOs decreases, thus having good biological effects and stability [22, 23]. Compared with other imaging methods such as MRI and CT, antisense imaging has the advantage that it detects specific gene expressions rather than anatomical changes [5]. Moreover, it can show the molecular level changes of the disease in the early stage non-invasively.

AMOs are negatively charged with electricity and their molecular weight is high, so their permeability of the membrane is low, and most AMOs cannot penetrate the cell. Whether the targeted nucleic acid molecules can specifically bind to the target gene and the uptake rate of the probe by the tumor are the keys to the success of targeted imaging technology [24]. Unmodified nucleic acid molecules are prone to degradation in vivo or in serum, resulting in the loss of activity. Certain chemical modification methods should be used to ensure the biological stability of oligonucleotides. Appropriate chemical modification can not only improve the hybridization affinity between the nucleic acid probe and target RNA, and improve its ability to resist nuclease degradation, but also slow down the plasma clearance rate of the nucleic acid probe and improve the ability to be absorbed by the organization. Previous studies have shown that the use of oligopeptide conjugated nucleic acids has many advantages. Different peptides have different biological characteristics after conjugation with nucleic acids, which can achieve targeted endocytosis [25]. Modifying the peptide at the 3'-end of RNA can improve the serum stability of the conjugate, and the nuclease resistance, and keep the silencing activity for a longer time [26]. After conjugating RNA with oligopeptide, other radionuclides can also be labeled. For example, AMOs radiolabeled iodine can be achieved after conjugating Tyr [27]. The correct design and modification of AMOs are also very impor-

tant to enhance their binding with miRNA specifically and firmly [28].

At present, the effect of ^{99m}Tc labeled nucleic acid is not ideal. In the past, many studies have constructed RNA radioactive labeled probes for antisense imaging through liposomes [29], transporters, membrane penetrating peptides, TAR binding peptides [30], SV40 nuclear localization sequences [31, 32], disulfide cyclic peptide IGF1 analogs [33, 34], dihydrotestosterone or nuclear localization peptides [35]. However, in these studies, there are many problems, such as complex labeling, low labeling efficiency, easy degradation, difficulty in penetrating the cell membrane, relatively high non-specific uptake of blood and other organs, and relatively low tumor uptake. Our research group has also coupled AMO with NHS-MAG$_3$, and the ^{99m}Tc labeling efficiency reached 97% [15]. In other studies, ^{99m}Tc was used to label AMO/cell-penetrating peptide PepFect6 (PF6), misAMO/PF6, and Naked AMO and commercial Lipofectamine 2000-based nano-particles. The labeling efficiency was 72.6%±1.42%, 72.4%± 2.71%, and 69.8%±3.69%, respectively [36]. However, the indirect labeling method has the disadvantages of long time, complex steps, many influencing factors, and nonspecific combination with serum proteins to form high polymers [4, 6, 37].

In this study, we successfully designed a new oligopeptide sequence GAGK for chelator-free radiolabeled AMO-21. The optimal labeling conditions were explored through labeling under different heating times and different SnCl$_2$·2H$_2$O concentrations. Our results show that the highest labeling efficiency can be obtained by labeling ^{99m}Tc-GAGK-AMO at the concentration of 1 mg/mL SnCl$_2$·2H$_2$O and heating for 30 min. Heating can shorten the labeling time and reduce the formation of colloids. By optimizing the reaction conditions, the final labeling efficiency reached 90.03%± 4.16%, which is enough for further purification for antisense imaging. The gel electrophoresis results showed that we successfully used GAGK to radiolabel AMO-21. The stability of radiolabeled AMO-21 in human fresh serum is very important, which seriously affects the imaging effect. The stability measurement results of this study showed that ^{99m}Tc-GAGK-AMO was only degraded slightly in serum within 12 hours

of incubation, indicating that GAGK-modified AMO-21 can remain stable in human serum. We assume that the peptide added on the 5'-end might play a role in the protection of this oligomer, which was similar to PNA. In addition, to improve binding stability and affinity, we modified 2'-O-methyl (2'-OMe) bases and phosphorothioate linkage bases at each end of AMO, which was mentioned in the material and method parts. Our study improved the problem of low labeling efficiency in previous AMO antisense imaging studies, while further verification of tumor uptake in vivo should be investigated.

Conclusion

We designed a new tetrapeptide GAGK to chemically modify AMO-21 which is targeting miRNA-21. After optimizing the reaction conditions, ^{99m}Tc radioactive labeling was achieved. This labeling method has high labeling efficiency and stable labeling, which provides an effective method for the application of miRNA-targeted imaging.

Disclosure of conflict of interest

None.

Address correspondence to: Lei Kang, Department of Nuclear Medicine, Peking University First Hospital, Beijing 100034, China. E-mail: kanglei@bjmu.edu.cn

References

[1] Soudy R, Chen C and Kaur K. Novel peptide-doxorubicin conjugates for targeting breast cancer cells including the multidrug resistant cells. J Med Chem 2013; 56: 7564-7573.

[2] Le Joncour V and Laakkonen P. Seek & destroy, use of targeting peptides for cancer detection and drug delivery. Bioorg Med Chem 2018; 26: 2797-2806.

[3] Skotland T. Molecular imaging: challenges of bringing imaging of intracellular targets into common clinical use. Contrast Media Mol Imaging 2012; 7: 1-6.

[4] Zhao X, Wang N, Ren X, Zhang J, Wang J, Han J, Jia L, Liu Y and Zhang Z. Preparation and evaluation of (99m)Tc-epidermal growth factor receptor (EGFR)-peptide nucleic acid for visualization of EGFR messenger RNA expression in malignant tumors. J Nucl Med 2014; 55: 1008-1016.

[5] Fu P, Shen B, Zhao C and Tian G. Molecular imaging of MDM2 messenger RNA with ^{99m}Tc-labeled antisense oligonucleotides in experimental human breast cancer xenografts. J Nucl Med 2010; 51: 1805-1812.

[6] Jiang Y, Gai Y, Long Y, Liu Q, Liu C, Zhang Y and Lan X. Application and evaluation of [(99m)Tc]-labeled peptide nucleic acid targeting microRNA-155 in breast cancer imaging. Mol Imaging 2020; 19: 1536012120916124.

[7] Liu G, Zhang S, He J, Liu N, Gupta S, Rusckowski M and Hnatowich DJ. The influence of chain length and base sequence on the pharmacokinetic behavior of ^{99m}Tc-morpholinos in mice. Q J Nucl Med 2002; 46: 233-243.

[8] Hernandez R, Orbay H and Cai W. Molecular imaging strategies for in vivo tracking of microRNAs: a comprehensive review. Curr Med Chem 2013; 20: 3594-3603.

[9] Stenvang J and Kauppinen S. MicroRNAs as targets for antisense-based therapeutics. Expert Opin Biol Ther 2008; 8: 59-81.

[10] Calin GA and Croce CM. MicroRNA signatures in human cancers. Nat Rev Cancer 2006; 6: 857-866.

[11] Lv W, Xu J, Wang X, Li X, Xu Q and Xin H. Bioengineered boronic ester modified dextran polymer nanoparticles as reactive oxygen species responsive nanocarrier for ischemic stroke treatment. ACS Nano 2018; 12: 5417-5426.

[12] Mohammadi R, Shokri B, Shamshirian D, Zarghi A and Shahhosseini S. Synthesis and biological evaluation of RGD conjugated with Ketoprofen/Naproxen and radiolabeled with [(99m)Tc] via N4(GGAG) for alphaVbeta3 integrin-targeted drug delivery. Daru 2020; 28: 87-96.

[13] Griffiths-Jones S, Grocock RJ, van Dongen S, Bateman A and Enright AJ. MiRBase: microRNA sequences, targets and gene nomenclature. Nucleic Acids Res 2006; 34: D140-144.

[14] Takahashi M, Yamada N, Hatakeyama H, Murata M, Sato Y, Minakawa N, Harashima H and Matsuda A. In vitro optimization of 2'-OMe-4'-thioribonucleoside-modified anti-microRNA oligonucleotides and its targeting delivery to mouse liver using a liposomal nanoparticle. Nucleic Acids Res 2013; 41: 10659-10667.

[15] Kang L, Fan Z, Sun H, Feng Y, Ma C, Yan P, Zhang C, Ma H, Hao P, Chen X, Zheng Z, Xu X and Wang R. Improved synthesis and biological evaluation of Tc-99m radiolabeled AMO for miRNA imaging in tumor xenografts. J Labelled Comp Radiopharm 2015; 58: 461-468.

[16] Dewanjee MK, Ghafouripour AK, Kapadvanjwala M, Dewanjee S, Serafini AN, Lopez DM and Sfakianakis GN. Noninvasive imaging of c-myc oncogene messenger RNA with indium-111-antisense probes in a mammary tumor-bearing mouse model. J Nucl Med 1994; 35: 1054-1063.

[17] Iyer AK and He J. Radiolabeled oligonucleotides for antisense imaging. Curr Org Synth 2011; 8: 604-614.

[18] Vanbilloen HP, De Roo MJ and Verbruggen AM. Complexes of technetium-99m with tetrapeptides containing one alanyl and three glycyl moieties. Eur J Nucl Med 1996; 23: 40-48.

[19] Liu S and Edwards DS. ^{99m}Tc-labeled small peptides as diagnostic radiopharmaceuticals. Chem Rev 1999; 99: 2235-2268.

[20] Lennox KA and Behlke MA. A direct comparison of anti-microRNA oligonucleotide potency. Pharm Res 2010; 27: 1788-1799.

[21] Kim G, Kim M, Lee Y, Byun JW, Hwang DW and Lee M. Systemic delivery of microRNA-21 antisense oligonucleotides to the brain using T7-peptide decorated exosomes. J Control Release 2020; 317: 273-281.

[22] Yu RZ, Geary RS, Monteith DK, Matson J, Truong L, Fitchett J and Levin AA. Tissue disposition of 2'-O-(2-methoxy) ethyl modified antisense oligonucleotides in monkeys. J Pharm Sci 2004; 93: 48-59.

[23] Fattal E and Bochot A. State of the art and perspectives for the delivery of antisense oligonucleotides and siRNA by polymeric nanocarriers. Int J Pharm 2008; 364: 237-248.

[24] Zhang HL, Wang P, Lu MZ, Zhang SD and Zheng L. C-Myc maintains the self-renewal and chemoresistance properties of colon cancer stem cells. Oncol Lett 2019; 17: 4487-4493.

[25] Juliano RL, Carver K, Cao C and Ming X. Receptors, endocytosis, and trafficking: the biological basis of targeted delivery of antisense and siRNA oligonucleotides. J Drug Target 2013; 21: 27-43.

[26] Fan X, Zhang Y, Liu X, He H, Ma Y, Sun J, Huang Y, Wang X, Wu Y, Zhang L and Yang Z. Biological properties of a 3',3''-bis-peptide-siRNA conjugate in vitro and in vivo. Bioconjug Chem 2016; 27: 1131-1142.

[27] Xian SZ, Chen Z, Huang WP, Zhao LN, Qiu YK, Hao P, Sun LX, Yang Q, Song LL and Kang L. One-step synthesis of a radioiodinated anti-microRNA-21 oligonucleotide for theranostics

in prostate tumor xenografts. Colloids Surf A Physicochem Eng Asp 2022; 649.

[28] Lennox KA and Behlke MA. Chemical modification and design of anti-miRNA oligonucleotides. Gene Ther 2011; 18: 1111-1120.

[29] Ren J, Zhang X, Cao J, Tian J, Luo J, Yu Y, Wang F and Zhao Q. Radiosynthesis of a novel antisense imaging probe targeting LncRNA HOTAIR in malignant glioma. BMC Cancer 2022; 22: 79.

[30] Soomets U, Hallbrink M and Langel U. Antisense properties of peptide nucleic acids. Front Biosci 1999; 4: D782-786.

[31] Cutrona G, Carpaneto EM, Ulivi M, Roncella S, Landt O, Ferrarini M and Boffa LC. Effects in live cells of a c-myc anti-gene PNA linked to a nuclear localization signal. Nat Biotechnol 2000; 18: 300-303.

[32] Branden LJ, Mohamed AJ and Smith CI. A peptide nucleic acid-nuclear localization signal fusion that mediates nuclear transport of DNA. Nat Biotechnol 1999; 17: 784-787.

[33] Pietrzkowski Z, Wernicke D, Porcu P, Jameson BA and Baserga R. Inhibition of cellular proliferation by peptide analogues of insulin-like growth factor 1. Cancer Res 1992; 52: 6447-6451.

[34] Basu S and Wickstrom E. Synthesis and characterization of a peptide nucleic acid conjugated to a D-peptide analog of insulin-like growth factor 1 for increased cellular uptake. Bioconjug Chem 1997; 8: 481-488.

[35] Boffa LC, Scarfi S, Mariani MR, Damonte G, Allfrey VG, Benatti U and Morris PL. Dihydrotestosterone as a selective cellular/nuclear localization vector for anti-gene peptide nucleic acid in prostatic carcinoma cells. Cancer Res 2000; 60: 2258-2262.

[36] Yang G, Zhao Y, Gong A, Miao W, Yan L, Nie P and Wang Z. Improved cellular delivery of antisense oligonucleotide for miRNA-21 imaging in vivo using cell-penetrating peptide-based nanoprobes. Mol Pharm 2021; 18: 787-795.

[37] Li YC, Tan TZ, Zheng JG and Zhang C. Antisense oligonucleotide labeled with technetium-99m using hydrazinonictinamide derivative and N-hydroxysuccinimidyl S-acetylmercaptoacetyltriglycline: a comparison of radiochemical behaviors and biological properties. World J Gastroenterol 2008; 14: 2235-2240.